**Received:** xxx **Accepted:** xxx **Published:** xxx.
DOI. xxxxxxx
Volume xxx, Issue xxx, p.p. 1-30: xxx
**Research Article**

Open Access

**Control and Optimization in Applied Mathematics - COAM**

# Optimal Control of a Predator–Prey Eco-Epidemic Model with Dual Prey Populations and Infectious Disease in One Species

**Mahnaz Abedini**[1], **Gorbanali Haghighatdoost**[1], **Hossein Kheiri**[2]✉

[1]Department of Mathematics, Azarbaijan Shahid Madani University, Tabriz, Iran
[2]Faculty of Mathematics, Statistics and Computer Science, University of Tabriz, Tabriz, Iran

✉ **Correspondence:**
Hossein Kheiri
**E-mail:**
h-kheiri@tabrizu.ac.ir

**How to Cite**
Abedini, M., Haghighatdoost, G., Kheiri, H. (2027). "Optimal control of a predator–prey eco-epidemic model with dual prey populations and infectious disease in one species". *Control and Optimization in Applied Mathematics*, X(x), 1-30. https://doi.org/10.30473/coam.2026.76520.1361

**Abstract.** This study develops and analyzes a four-compartment predator–prey model incorporating disease dynamics and optimal control. The first prey population follows logistic growth and is susceptible to infection, whereas the second prey population remains disease-free and exhibits greater competitive ability. The model incorporates an epidemic process within the first prey population and considers two control measures: reducing disease transmission and treating or removing infected individuals. We investigate the resulting system theoretically to assess the effects of these interventions on disease prevalence, prey persistence, predator dynamics, and ecosystem stability. In particular, stability analysis, sensitivity analysis, and optimal control theory are employed to characterize the model dynamics and identify the most influential parameters. The results indicate that the carrying capacity ($k$), infection rate ($\gamma$), and disease-induced mortality rate ($\mu$) play major roles in determining the persistence of infection. Moreover, the optimal isolation ($u_1$) and treatment ($u_2$) strategies substantially reduce disease prevalence, increase the healthy prey population, and promote predator stability compared with the uncontrolled scenario. Numerical simulations further demonstrate the effectiveness of the proposed control strategies in mitigating infection and maintaining ecological balance. These findings demonstrate that the model provides a unified framework for examining the interactions between heterogeneous prey populations, disease transmission, predation, and targeted control interventions.

**Keywords.** Predator-prey model, Prey infection, Optimal control, Stability analysis, Sensitivity analysis.

**MSC.** 49L20; 00A71.

## 1 Introduction

The mathematical modeling and analysis of dynamic phenomena, particularly the spread and control of infectious diseases, have become important areas of research in biomathematics, with significant contributions to our understanding of disease transmission and control [5, 13]. For instance, [6] investigated a multi-group epidemic model and examined optimal strategies for controlling an infectious disease.

Predator-prey interactions are central to ecosystem stability and biodiversity conservation. When prey species become infected with a disease, the system dynamics become markedly more complex: disease modifies prey growth and mortality rates, alters contact and predation-access patterns, and thus affects not only the prey population but also the predator, and overall community structure. This has motivated the development of eco-epidemiological models, in which ecological interactions (such as predation and competition) are coupled with epidemiological processes (such as disease transmission and recovery) to yield richer insights into population dynamics, disease control, and ecosystem management [4, 9, 14].

Early eco-epidemiological models generally considered a single prey population divided into susceptible and infected classes alongside a predator species. A notable example is the study by Mukhopadhyay and Bhattacharyya, which introduced predator switching behavior between susceptible and infected prey, highlighting how predator preferences can modify disease dynamics within prey populations [17]. Similarly, Greenhalgh et al. developed a model incorporating a ratio-dependent functional response, allowing predators to distinguish between healthy and infected prey, further enriching the understanding of predator-prey-disease interactions [10].

More recent research has expanded the framework by incorporating fractional-order dynamics, spatial diffusion, Allee effects, fear effects, prey refuge, and migration to capture more realistic ecological complexities. For instance, an eco-epidemiological model accounting for the impact of fear on prey demonstrated how predator-induced fear alters infection dynamics and prey behavior [10]. Further advancing the field, the application of optimal control theory to an eco-epidemiological reaction-diffusion model was explored, introducing spatial interventions such as isolation and treatment to optimize disease control while preserving ecosystem stability [12, 16, 19].

Despite significant advances, several important gaps remain in the eco-epidemiological modeling literature. Many existing models assume symmetric disease effects or focus on a single prey species, which limits their ecological realism in natural systems where multiple prey species compete, with only one species harboring infection while others remain disease-free [10, 17]. Moreover, although optimal control methods have been applied in some eco-epidemiological settings, few studies comprehensively integrate multiple prey populations,

asymmetric disease structuring, and dual intervention strategies, such as transmission reduction and treatment, within a unified control framework [7, 22].

In this study, we address these limitations by developing a predator-prey model comprising two prey populations: one infected (subdivided into susceptible and infected classes) and the other disease-free yet competitively superior. We introduce two time-dependent control variables aimed at (i) reducing disease transmission among the infected prey population and (ii) treating or removing infected individuals. Employing Pontryagin's Maximum Principle, we establish the existence of optimal controls and conduct rigorous stability analysis, complemented by numerical simulations and parameter sensitivity investigations.

The novelty of our work lies in the integration of dual prey populations, heterogeneous infection dynamics, and dual intervention mechanisms, all within a cohesive eco-epidemiological and optimal control framework.

The subsequent sections of this paper are structured as follows: Section 2 details the mathematical formulation of the predator-prey model, elucidating key assumptions and equations. In Section 3, the quality behavior of the model is discussed. Section 4 deals the sensitivity analysis of the infectious population of model respect to parameters of model. In Section 5 presents the existence of optimal controls and derives the necessary conditions using Pontryagin's Maximum Principle; Section 6, the numerical methods used for simulations are outlined, along with the model parameterizations. Section 7 is devoted to conclusion of the paper.

## 2 Description of Model

In this section, we construct a prey-predator model to look at the effects of predation. We assume that the following hypothesis holds for our model.

(i) The first prey population, denoted as $s_1(t)$, grows logistically with an intrinsic growth rate of $r$ and an environmental carrying capacity of $k$. Mass-action is assumed between susceptibles and infecteds in the first prey.

(ii) The infectious population of the first prey, denoted as $I(t)$.

(iii) The second prey population, denoted as $s_2(t)$, is assumed to experience a constant growth rate. This prey species is considered stronger than the first and remains free of infectious disease. As a result, the predator preferentially targets the first prey, thereby providing an indirect advantage to the second prey-an assumption that underpins this dynamic.

(iv) The predator population, denoted as $x(t)$, is assumed to grow exponentially with a negative growth rate. Additionally, predators are not affected by infection when consuming

infected prey. Mass-action is assumed between the predator population and the prey population.

Figure 1, illustrates the interactions among three prey groups $s_1, I, s_2$ and a predator $x$. This diagram highlights the processes of predation, disease transmission, and the predator's impact on prey populations.

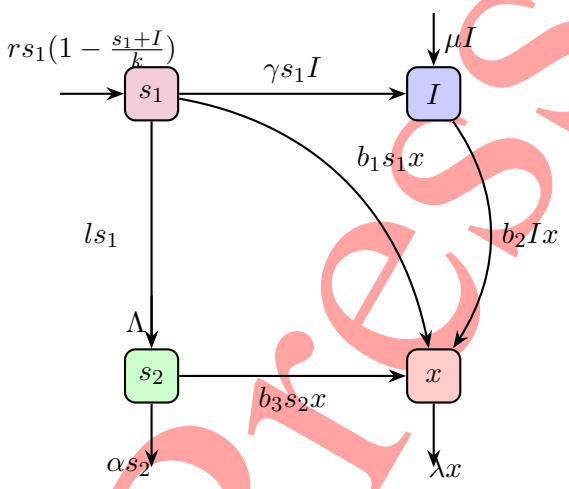


**Figure 1:** Schematic diagram showing the interactions among healthy preys $(s_1, s_2)$, infected prey $(I)$, and the predator $(x)$.

Considering the above assumptions, we apply the following dynamic model for predator and prey populations:

$$\begin{aligned}
\frac{ds_1}{dt} &= rs_1(1-\frac{s_1+I}{k}) - b_1 s_1 x - \gamma s_1 I,\\
\frac{dI}{dt} &= \gamma s_1 I - b_2 Ix - \mu I,\\
\frac{ds_2}{dt} &= \Lambda - \alpha s_2 - b_3 s_2 x + ls_1,\\
\frac{dx}{dt} &= -\lambda x + e_1 b_1 s_1 x + e_2 b_2 Ix + e_3 b_3 s_2 x,
\end{aligned} \tag{1}$$

with initial conditions:

$$s_1(0) \geq 0,\ I(0) \geq 0,\ s_2(0) \geq 0,\ x(0) \geq 0. \tag{2}$$

Description of parameters are given in Table 1.

**Table 1:** Definitions and descriptions of the parameters for model (1).

| Parameter | Description |
|---|---|
| $r$ | Logistic growth rate of the first healthy prey population |
| $k$ | Environmental carrying capacity |
| $\gamma$ | Infection rate of the first prey population |
| $\mu$ | Mortality rate of the first infected prey |
| $\Lambda$ | Constant growth rate of the second prey |
| $\alpha$ | Natural mortality rate of the second prey |
| $l$ | Intensity of the indirect effect |
| $\lambda$ | Natural mortality rate of the predator |
| $b_i,\ i = 1, 2, 3$ | Predation rates of the first susceptible, infected, and second prey by predators |
| $e_i,\ i = 1, 2, 3$ | Conversion efficiencies |

## 3 Qualitative Behavior of the system

### 3.1 Existence, Uniqueness, Positivity, and Boundedness of Solutions

**Theorem 1** (Existence and Uniqueness)**.** Consider system (1) with a nonnegative initial condition

$$(s_1(0), I(0), s_2(0), x(0)) \in \mathbb{R}^4_+.$$

Then there exists a unique solution

$$(s_1(t), I(t), s_2(t), x(t)),$$

defined on a maximal interval $[0, T)$ with $T > 0$. Moreover, the solution depends continuously on the initial condition.

*Proof.* System (1) can be written in the compact vector form

$$\frac{d\mathbf{Y}}{dt} = \mathbf{F}(\mathbf{Y}),$$

where $\mathbf{Y} = (s_1, I, s_2, x) \in \mathbb{R}^4$ and $\mathbf{F} = (f_1, f_2, f_3, f_4)$ is defined by

$$\begin{aligned}
f_1(\mathbf{Y}) &= r s_1 \left(1 - \frac{s_1 + I}{k}\right) - b_1 s_1 x - \gamma s_1 I, \\
f_2(\mathbf{Y}) &= \gamma s_1 I - b_2 I x - \mu I, \\
f_3(\mathbf{Y}) &= \Lambda - \alpha s_2 - b_3 s_2 x + l s_1, \\
f_4(\mathbf{Y}) &= -\lambda x + e_1 b_1 s_1 x + e_2 b_2 I x + e_3 b_3 s_2 x.
\end{aligned}$$

Since each component $f_i(\mathbf{Y})$ is a polynomial function of the state variables, it follows that $\mathbf{F} \in C^1(\mathbb{R}^4)$. Hence, $\mathbf{F}$ is locally Lipschitz continuous on $\mathbb{R}^4$.

Therefore, by the Picard–Lindelöf theorem (Cauchy–Lipschitz theorem)[20] , for any initial condition $\mathbf{Y}(0) = \mathbf{Y}_0 \in \mathbb{R}^4_+$, there exists a unique local solution $\mathbf{Y}(t)$ defined on some interval $[0, T)$ with $T > 0$. Moreover, the solution depends continuously on the initial data. This completes the proof. □

**Theorem 2** (Positivity)**.** All solutions of system (1) starting in $\mathbb{R}^4_+$ remain non-negative for all $t \geq 0$.

*Proof.* On the hyperplanes of region $\Omega_+$ we have

$$\dot{s_1}|_{s_1=0} = 0, \tag{3}$$

$$\dot{I}|_{I=0} = 0, \tag{4}$$

$$\dot{s_2}|_{s_2=0} = \Lambda + ls_1 \geq 0, \tag{5}$$

$$\dot{x}|_{x=0} = 0. \tag{6}$$

By choosing the initial condition from region $\Omega_+$, relations (3) to (6) show that the hyperplanes corresponding to the state variables led the phase trajectories into region $\Omega_+$ and it is not possible for any of the state variables to become negative. □

Since $s_1(t), I(t) \leq N_1(t) \leq K$ and $s_2(t) \leq S_2$ for all $t \geq 0$, we obtain the following estimate:

$$e_1 b_1 s_1(t) + e_2 b_2 I(t) \leq \max\{e_1 b_1, e_2 b_2\} K.$$

Define

$$M := \max\{e_1 b_1, e_2 b_2\} K + e_3 b_3 S_2.$$

Then, for all $t \geq 0$, the function $\rho(t) = -\lambda + e_1 b_1 s_1(t) + e_2 b_2 I(t) + e_3 b_3 s_2(t)$ satisfies

$$\rho(t) \leq M - \lambda.$$

From the fourth equation of system (1), $\frac{dx}{dt} = \rho(t)x(t)$, direct integration yields

$$x(t) = x(0) \exp\left(\int_0^t \rho(\tau)\, d\tau\right) \leq x(0) e^{(M-\lambda)t}, \qquad \forall t \geq 0.$$

If $\lambda \geq M$, then $M - \lambda \leq 0$, which implies that $x(t) \leq x(0)$ for all $t \geq 0$. Moreover, in this case $x(t)$ decays exponentially to zero as $t \to \infty$. Consequently, $x(t)$ is uniformly bounded on $[0, \infty)$. This completes the proof of uniform boundedness of all solutions.

**Theorem 3** (Uniform Boundedness)**.** All solutions of system (1) initiating in $\mathbb{R}^4_+$ are uniformly bounded for all $t \geq 0$.

*Proof.* Let $N_1(t) = s_1(t) + I(t)$. Adding the first two equations in (1):

$$\frac{dN_1}{dt} \leq rs_1\left(1 - \frac{N_1}{k}\right) \leq rN_1 - \frac{r}{k}N_1^2.$$

For $N_1(t_0) > k$, we have $\frac{dN_1}{dt} < 0$, which means $N_1$ decreases. Therefore, $N_1(t) < N_1(t_0)$, for all $t > t_0$. Then the $N_1$ will be bounded.
If $N_1(t_0) \leq k$, then $N_1(t) \leq k$ for all $t \geq t_0$. Therefore

$$N_1(t) \leq \max\{N_1(t_0), k\} = K.$$

Then the state variables $s_1$, and $I$ are boundedness.

From the third equation and the boundedness of $s_1, I$ we have:

$$\frac{ds_2}{dt} \leq \Lambda - \alpha s_2 + lK \qquad \Rightarrow \qquad \frac{ds_2}{dt} + \alpha s_2 \leq \Lambda + lK.$$

This is a first-order linear differential inequality. Using the integrating factor $e^{\alpha t}$, we obtain:

$$\frac{d}{dt}(s_2 e^{\alpha t}) \leq (\Lambda + lK)e^{\alpha t}.$$

Integrating yields:

$$s_2(t)e^{\alpha t} - s_2(0) \leq \frac{\Lambda + lK}{\alpha}(e^{\alpha t} - 1).$$

Then

$$s_2(t) \leq s_2(0)e^{-\alpha t} + \frac{\Lambda + lK}{\alpha}(1 - e^{-\alpha t}).$$

Therefore:

$$s_2(t) \leq \max\{s_2(0), \frac{\Lambda + lK}{\alpha}\} = S_2 \quad \text{for all } t \geq 0.$$

Therefore, the state variable $s_2$ is boundedness.

Since $s_1(t), I(t) \leq N_1(t) \leq K$ and $s_2(t) \leq S_2$, we have:

$$e_1b_1s_1(t) + e_2b_2I(t) \leq \max\{e_1b_1, e_2b_2\}K.$$

Define

$$\bar{M} := \max\{e_1b_1, e_2b_2\}K + e_3b_3S_2.$$

Then for all $t \geq 0$:

$$\rho(t) = -\lambda + e_1b_1s_1(t) + e_2b_2I(t) + e_3b_3s_2(t) \leq \bar{M} - \lambda.$$

From $\frac{dx}{dt} = \rho(t)x(t)$, we obtain:

$$x(t) = x(0)\exp\left(\int_0^t \rho(\tau)\,d\tau\right) \leq x(0)e^{(\bar{M}-\lambda)t}.$$

If $\lambda \geq \bar{M}$, then $\bar{M} - \lambda \leq 0$, which implies that $x(t) \leq x(0)$ for all $t \geq 0$. Moreover, in this case $x(t)$ decays exponentially to zero as $t \to \infty$. Consequently, $x(t)$ is uniformly bounded on $[0, \infty)$. This completes the proof of uniform boundedness of all solutions. □

### 3.2 Equilibrium Points of the System

In this section, we determine the equilibrium points of the model and derive the conditions for their existence. To this end, we set the right-hand sides of system (1) equal to zero and solve the resulting algebraic system. Six nonnegative equilibrium points are obtained, namely,

$$E_1 = (0, 0, s_2^*, 0), \quad E_2 = (s_1^*, 0, s_2^*, 0), \quad E_3 = (0, 0, s_2^*, x^*),$$

$$E_4 = (s_1^*, 0, s_2^*, x^*), \quad E_5 = (s_1^*, I^*, s_2^*, 0),$$

and the coexistence equilibrium

$$E_6 = (s_1^*, I^*, s_2^*, x^*).$$

The corresponding existence conditions for these equilibrium points are given below.

(i) **Existence of** $E_1 = (0, 0, s_2^*, 0)$

Let $s_1 = 0, I = 0$ and $x = 0$. Solving the system (1) gives: $\Lambda - \alpha s_2 = 0$. Then, we have $s_2^* = \dfrac{\Lambda}{\alpha}$. Therefore, the equilibrium point $E_1 = (0, 0, \dfrac{\Lambda}{\alpha}, 0)$ is established unconditionally.

(ii) **Existence of** $E_2 = (s_1^*, 0, s_2^*, 0)$

Let $I = 0$ and $x = 0$. So, solving the system (1) gives: $rs_1(1 - \dfrac{s_1}{k}) = 0$ and $\Lambda - \alpha s_2 + ls_1 = 0$. From this we have $s_1^* = k$ and $s_2^* = \dfrac{\Lambda + lk}{\alpha}$. Thus, the equilibrium point $E_2 = (k, 0, \dfrac{\Lambda + lk}{\alpha}, 0)$ always exists.

(iii) **Existence of** $E_3 = (0, 0, s_2^*, x^*)$

Let $s_1 = 0$ and $I = 0$. Solving the system (1) results:

$$\Lambda - \alpha s_2 - b_3 s_2 x = 0 \qquad and \qquad x(-\lambda + e_3 b_3 s_2) = 0.$$

Therefore, the equilibrium point $E_3 = (0, 0, \dfrac{\lambda}{e_3 b_3}, \dfrac{\Lambda e_3 b_3 - \alpha\lambda}{\lambda b_3})$ exists provided,

$$\Lambda e_3 b_3 - \alpha\lambda > 0.$$

(iv) **Existence of** $E_4 = (s_1^*, 0, s_2^*, x^*)$

Let $I = 0$. Then, system (1) takes the following form:

$$\begin{aligned} &s_1 \left( r \left( 1 - \frac{s_1}{k} \right) - e_1 b_1 x \right) = 0, \\ &\Lambda - \alpha s_2 - b_3 s_2 x + l s_1 = 0, \end{aligned} \tag{7}$$

$$x\left(-\lambda + e_1 b_1 s_1 + e_3 b_3 s_2\right) = 0.$$

By straightforward calculations, we obtain:

$$x = \frac{r}{e_1 b_1}\left(1 - \frac{s_1}{k}\right), \qquad s_2 = \frac{\lambda - e_1 b_1 s_1}{e_3 b_3}.$$

Substituting these expressions into the second equation of (7), we derive:

$$-\frac{r e_1}{k e_3} s_1^2 + \left(\frac{\alpha e_1 k b_1}{e_3 b_3} + \frac{r(e_1 b_1 k + \lambda)}{e_1 b_1 e_3 k} + l\right) s_1 + (\Lambda - \frac{\alpha\lambda}{e_3 b_3} - \frac{r\lambda}{e_1 b_1 e_3}) = 0. \tag{8}$$

We can rewrite equation (8) in the quadratic form:

$$A s_1^2 + B s_1 + C = 0, \tag{9}$$

where

$$A = -\frac{r e_1}{k e_3}, \quad B = +\left(\frac{\alpha e_1 k b_1}{e_3 b_3} + \frac{r(e_1 b_1 k + \lambda)}{e_1 b_1 e_3 k} + l\right), \quad C = (\Lambda - \frac{\alpha\lambda}{e_3 b_3} - \frac{r\lambda}{e_1 b_1 e_3}).$$

Here, $A < 0$, $B > 0$, and $C$ will be negative provided that

$$\Lambda < \frac{\alpha\lambda}{e_3 b_3} + \frac{r\lambda}{e_3 b_1}. \tag{10}$$

Let the roots of equation (9) be $s_{11}^*$ and $s_{12}^*$. Then,

$$s_{11}^* + s_{12}^* = -\frac{B}{A} > 0, \quad s_{11}^* s_{12}^* = \frac{C}{A} < 0,$$

where it is assumed that $s_{11}^* > s_{12}^*$.

If condition (10) holds, both $s_{11}^*$ and $s_{12}^*$ exist. Otherwise, only $s_{11}^*$ exists as a valid root.

(v) **Existence of** $E_5 = (s_1^*, I^*, s_2^*, 0)$

At the predator-free equilibrium, we set $x = 0$ in system (1). This reduces the system to:

$$\begin{aligned} (r\left(1 - \frac{s_1 + I}{k}\right) - \gamma I) &= 0, \\ (\gamma s_1 - \mu) I &= 0, \\ \Lambda - \alpha s_2 + l s_1 &= 0. \end{aligned}$$

From the second equation, since $I \neq 0$ at this equilibrium, we obtain $s_1^* = \frac{\mu}{\gamma}$. Substituting $s_1^*$ into the first equation and solving for $I$ yields:

$$I^* = \frac{r(\gamma k - \mu)}{\gamma(\gamma k + r)}.$$

Substituting $s_1^*$ into the third equation and solving for $s_2$ gives:

$$s_2^* = \frac{\Lambda + ls_1^*}{\alpha} = \frac{\Lambda\gamma + l\mu}{\alpha\gamma}.$$

Thus, the equilibrium point is explicitly given by: In this case, we have

$$E_5 = (\frac{\mu}{\gamma}, \frac{r(\gamma k - \mu)}{\gamma(\gamma k + r)}, \frac{\Lambda\gamma + l\mu}{\alpha\gamma}, 0).$$

This equilibrium point exists if,

$$\gamma k > \mu.$$

(vi) **Existence of** $E_6 = (s_1^*, I^*, s_2^*, x^*)$

The coexistence equilibrium is obtained by setting the right-hand sides of system (1) to zero,Therefore, we have:

$$\begin{aligned} r(1 - \frac{s_1 + I}{k}) - b_1 x - \gamma I &= 0, \\ \gamma s_1 - b_2 x - \mu &= 0, \\ \Lambda - \alpha s_2 - b_3 s_2 x + l s_1 &= 0, \\ -\lambda + e_1 b_1 s_1 + e_2 b_2 I + e_3 b_3 s_2 &= 0. \end{aligned} \tag{11}$$

In this case, the expressions for $x$, $I$, and $s_2$ are derived from the second, first, and last equations of system (11), respectively, and are given by:

$$\begin{aligned} x &= \frac{\gamma s_1 - \mu}{b_2}, \\ I &= \frac{((-\gamma s_1 + \mu)b_1 + r b_2)k - r b_2 s_1}{b_2(\gamma k + r)}, \\ s_2 &= \frac{\big(-e_2 r b_2 + \big((\gamma s_1 - \mu)e_2 - s_1 \gamma e_1\big)b_1 + \gamma\lambda\big)k + r\big(-b_1 e_1 s_1 + b_2 e_2 s_1 + \lambda\big)}{(\gamma k + r)e_3 b_3}. \end{aligned}$$

Substituting these values in

$$\Lambda - \alpha s_2 - b_3 s_2 x + l s_1 = 0,$$

gives:

$$A s_1^2 + B s_1 + C = 0, \tag{12}$$

where,

$$A = \frac{(k b_1(e_1 - e_2)\gamma + r(e_1 b_1 - e_2 b_2))\gamma}{b_2(\gamma k + r)e_3},$$

$$B = \frac{1}{b_2(\gamma k + r)e_3 b_3}\Big[\Big(\big(k(le_3 + re_2)\gamma + r(le_3 + \mu e_2)\big)b_2 - k\lambda\gamma^2 + \big(-\mu b_1(e_1 - 2e_2)k - \lambda r\big)\gamma - e_1 r\mu b_1\Big)b_3 + b_2\Big(-e_2 r b_2 + \big(k(e_1 - e_2)\gamma + e_1 r\big)b_1\Big)\alpha\Big],$$

$$C = -\frac{(-\alpha b_2 + \mu b_3)\big((\mu b_1 e_2 + r b_2 e_2 - \gamma\lambda)k - \lambda r\big)}{b_2(\gamma k + r)e_3 b_3} + \Lambda.$$

To determine the existence of this equilibrium point, By considering (12) For any real equilibrium to exist, the discriminant must be non-negative:

$$B^2 - 4AC \geq 0.$$

The point $E_6$ corresponds to a positive root of this equation. the sum of the roots is $-\frac{B}{A}$ and their product is $\frac{C}{A}$.

$$-\frac{B}{A} > 0 \quad \Rightarrow \quad AB < 0.$$

Thus, the necessary conditions for the existence of $E_6$ are:

$$B^2 - 4AC \geq 0, \qquad AB < 0. \tag{13}$$

Under condition (13), the sign of $AC$ determines the number of positive roots: if $AC > 0$, there are two positive roots, and if $AC < 0$, there is exactly one positive root.

### 3.3 Local stability of the free-disease equilibrium points

The Jacobian matrix $J$ of system (1) with respect to the variables $(s_1, I, s_2, x)$ is:

$$J = \begin{pmatrix} r\left(1 - \frac{2s_1 + I}{k}\right) - b_1 x - \gamma I & -\frac{rs_1}{k} - \gamma s_1 & 0 & -b_1 s_1 \\ \gamma I & \gamma s_1 - b_2 x - \mu & 0 & -b_2 I \\ l & 0 & -\alpha - b_3 x & -b_3 s_2 \\ e_1 b_1 x & e_2 b_2 x & e_3 b_3 x & -\lambda + e_1 b_1 s_1 + e_2 b_2 I + e_3 b_3 s_2 \end{pmatrix}.$$

(i) The Jacobian matrix at the equilibrium point $E_1 = (0, 0, \frac{\Lambda}{\alpha}, 0)$ has eigenvalues :

$$-\alpha, \quad -\mu, \quad r, \quad \frac{e_3 b_3 \Lambda - \lambda\alpha}{\alpha}.$$

Since $r > 0$, this equilibrium point is always unstable.

(ii) The Jacobian matrix evaluated at the equilibrium point $E_2 = (k, 0, \frac{\Lambda + lk}{\alpha}, 0)$ possesses negative eigenvalues, provided that the following conditions are satisfied:

$$\mu > \gamma k,$$
$$\lambda\alpha > (\alpha k b_1 e_1) + (k l b_3 e_3) + (\Lambda b_3 e_3). \tag{14}$$

(iii) The eigenvalues of the Jacobian matrix at the equilibrium point

$$E_3 = (0, 0, \frac{\lambda}{e_3 b_3}, \frac{\Lambda e_3 b_3 - \alpha\lambda}{\lambda b_3}),$$

are given by:

$$\lambda_1 = \frac{\alpha\lambda b_1 + \lambda r b_3 - \Lambda e_3 b_1 b_3}{\lambda b_3},$$
$$\lambda_2 = \frac{\alpha\lambda b_2 - \lambda b_3\mu - \Lambda e_3 b_2 b_3}{\lambda b_3},$$
$$\lambda_{3,4} = \frac{-B \pm \sqrt{C}}{2\lambda},$$

where

$$B = \Lambda e_3 b_3, \qquad C = B^2 - 4B\lambda^2 + 4\alpha\lambda^3 = 4\alpha\lambda^3 - 4\lambda^2\Lambda e_3 b_3 + \Lambda^2 e_3^2 b_3^2,$$

Then, the equilibrium point $E_3$ is locally asymptotically stable if the following condition holds:

$$\alpha\lambda b_1 + \lambda r b_3 < \Lambda e_3 b_1 b_3,$$
$$\alpha\lambda b_2 - \lambda b_3\mu - \Lambda e_3 b_2 b_3 < 0,$$

For the eigenvalues $\lambda_{3,4} = \frac{-B \pm \sqrt{C}}{2\lambda}$, Two cases arise based on the sign of $C$. If $C \geq 0$, the eigenvalues are real and given by $\lambda_3 = \frac{-B + \sqrt{C}}{2\lambda}$ and $\lambda_4 = \frac{-B - \sqrt{C}}{2\lambda}$. The eigenvalue $\lambda_4$ is always negative provided $B > 0$, since $-B - \sqrt{C} < 0$. For $\lambda_3$ to be negative, we require $-B + \sqrt{C} < 0$, which simplifies to $\sqrt{C} < B$ or equivalently $C < B^2$. Thus, for $C \geq 0$, the conditions $B > 0$and $C < B^2$ ensure both eigenvalues are negative.

(iv) For the equilibrium point $E_4 = (s_1^*, 0, s_2^*, x^*)$ Jacobian matrix is given:

$$J(E_4) = \begin{pmatrix} -\frac{rs_1}{k} & -\frac{rs_1}{k} - \gamma s_1 & 0 & -b_1 s_1 \\ 0 & \gamma s_1 - b_2 x - \mu & 0 & 0 \\ l & 0 & -b_3 x - \alpha & -b_3 s_2 \\ e_1 b_1 x & e_2 b_2 x & e_3 b_3 x & 0 \end{pmatrix}.$$

By assuming

$$J_{11} = -\frac{rs_1}{k}, \quad J_{12} = -\frac{rs_1}{k} - \gamma s_1, \quad J_{14} = -b_1 s_1,$$
$$J_{22} = \gamma s_1 - b_2 x - \mu, \quad J_{31} = l, \quad J_{33} = -b_3 x - \alpha,$$
$$J_{34} = -b_3 s_2, \quad J_{41} = e_1 b_1 x, \quad J_{42} = e_2 b_2 x,$$
$$J_{43} = e_3 b_3 x.$$

After straightforward calculations, the characteristic equation of the Jacobian matrix $J(E_4)$ is obtained as:

$$\lambda^4 + A_1'\lambda^3 + A_2'\lambda^2 + A_3'\lambda + A_4', \tag{15}$$

where

$$A_1' = -J_{11} - J_{22} - J_{33},$$
$$A_2' = J_{11}J_{22} + J_{11}J_{33} - J_{14}J_{41} + J_{22}J_{33} - J_{34}J_{43},$$
$$A_3' = -J_{11}J_{22}J_{33} + J_{11}J_{34}J_{43} + J_{14}J_{22}J_{41} + J_{14}J_{33}J_{41} - J_{43}J_{31}J_{41},$$
$$A_4' = -J_{11}J_{22}J_{34}J_{43} + J_{31}J_{14}J_{43}J_{22} - J_{14}J_{22}J_{33}J_{41}.$$

By Routh-Hurwitz criterionn [1], the equilibrium point $E_4$ is locally asymptotically stable provided the following conditions hold:

$$A_i' > 0, \quad i = 1, \cdots, 4, \quad \text{and} \quad A_1'(A_2'A_3' - A_1'A_4') - A_3'^2 > 0. \tag{16}$$

### 3.4 Local Stability of the Disease-affected Equilibrium Points

(v) The Jacobian matrix evaluated at the equilibrium point

$$E_5 = (\frac{\mu}{\gamma}, \frac{r(\gamma k - \mu)}{\gamma(\gamma k + r)}, \frac{\Lambda\gamma + l\mu}{\alpha\gamma}, 0).$$

takes the form:

$$J(E_5) = \begin{pmatrix} M_{11} & M_{12} & 0 & M_{14} \\ M_{21} & M_{22} & 0 & M_{24} \\ M_{31} & 0 & M_{33} & M_{34} \\ 0 & 0 & 0 & M_{44} \end{pmatrix},$$

where

$$M_{11} = r(1 - \frac{s_1 + I}{k}) - \frac{rs_1}{k} - \gamma I, \quad M_{12} = \frac{-rs_1}{k} - \gamma s_1,$$
$$M_{14} = -b_1 s_1, \quad M_{21} = \gamma I, \quad M_{22} = \gamma s_1 - \mu,$$

$$M_{24} = -b_2 I, \qquad M_{31} = l, \qquad M_{33} = -\alpha,$$
$$M_{34} = -b_3 s_2, \qquad M_{44} = e_1 b_1 s_1 + e_2 b_2 I + e_3 b_3 s_2 - \lambda.$$

Through straightforward computation, the characteristic equation of the Jacobian matrix $J(E_5)$ can be expressed as:

$$P(\lambda) = \lambda^4 + B_1\lambda^3 + B_2\lambda^2 + B_3\lambda + B_4, \tag{17}$$

where

$$B_1 = -M_{44} - M_{33} - M_{22} - M_{11},$$
$$B_2 = M_{11}M_{22} + M_{11}M_{33} + M_{11}M_{44} - M_{12}M_{21} + M_{22}M_{33} + M_{22}M_{44} + M_{33}M_{44},$$
$$B_3 = -M_{11}M_{22}M_{33} - M_{11}M_{22}M_{44} - M_{11}M_{33}M_{44} + M_{12}M_{21}M_{33} + M_{12}M_{21}M_{44} - M_{22}M_{33}M_{44},$$
$$B_4 = M_{44}M_{33}(M_{11}M_{22} - M_{12}M_{21}).$$

Applying the Routh-Hurwitz criterion [1], to the equilibrium point $E_5$ is locally asymptotically stable if and only if the following conditions hold:

$$B_1 > 0, \quad B_3 > 0, \quad B_4 > 0, \qquad B_1\left(B_2B_3 - B_1B_4\right) - B_3^2 > 0. \tag{18}$$

These conditions translate into the following constraints on the parameters $M_{ij}$:

$$-M_{44} - M_{33} - M_{22} - M_{11} > 0,$$
$$-M_{11}M_{22}M_{33} - M_{11}M_{22}M_{44} - M_{11}M_{33}M_{44} + M_{12}M_{21}M_{33} + M_{12}M_{21}M_{44} - M_{22}M_{33}M_{44} > 0,$$
$$M_{44}M_{33}\left(M_{11}M_{22} - M_{12}M_{21}\right) > 0,$$
$$B_1\left(B_2B_3 - B_1B_4\right) - B_3^2 > 0.$$

The last inequality represents a complicated algebraic condition that ensures all eigenvalues have negative real parts. Due to its length and complexity, it is not expanded explicitly here, but it must be satisfied for stability.

(vi) For the equilibrium point $E_6 = (s_1^*, I^*, s_2^*, x^*)$ we have:

$$J(E_6) = \begin{pmatrix} J_{11} & J_{12} & 0 & J_{14} \\ J_{21} & 0 & 0 & J_{24} \\ J_{31} & 0 & J_{33} & J_{34} \\ J_{41} & J_{42} & J_{43} & 0 \end{pmatrix},$$

where

$$J_{11} = -\frac{rs_1}{k}, \quad J_{12} = \frac{-rs_1}{k} - \gamma s_1, \quad J_{14} = -b_1 s_1, \quad J_{21} = \gamma I,$$
$$J_{24} = -b_2 I, \quad J_{31} = l, \quad J_{33} = -b_3 x - \alpha,$$
$$J_{34} = -b_3 s_2, \quad J_{41} = e_1 b_1 x, \quad J_{42} = e_2 b_2 x, \quad J_{43} = e_3 b_3 x.$$

Computing the characteristic equation of $J(E_6)$ yields:

$$\lambda^4 + D_1\lambda^3 + D_2\lambda^2 + D_3\lambda + D_4 = 0, \tag{19}$$

where

$$\begin{aligned}
D_1 &= -J_{11} - J_{33}, \\
D_2 &= J_{11}J_{33} - J_{12}J_{21} - J_{14}J_{41} - J_{24}J_{42} - J_{34}J_{43}, \\
D_3 &= J_{11}J_{24}J_{42} + J_{11}J_{34}J_{43} + J_{12}J_{21}J_{33} - J_{12}J_{24}J_{41} - J_{14}J_{21}J_{42} \\
&- J_{14}J_{31}J_{43} + J_{14}J_{33}J_{41} - J_{24}J_{32}J_{43} + J_{24}J_{33}J_{42} \\
D_4 &= J_{11}J_{24}J_{32}J_{43} - J_{11}J_{24}J_{33}J_{42} + J_{12}J_{21}J_{34}J_{43} - J_{12}J_{24}J_{31}J_{43} \\
&+ J_{12}J_{24}J_{33}J_{41} - J_{14}J_{21}J_{32}J_{43} + J_{14}J_{21}J_{33}J_{42}.
\end{aligned}$$

The characteristic polynomial of the Jacobian matrix at $E_6$ is given by (19). Applying the Routh-Hurwitz criterion, the necessary and sufficient conditions for local asymptotic stability of $E_6$ are:

$$D_1 > 0, \quad D_3 > 0, \quad D_4 > 0, \quad D_1(D_2D_3 - D_1D_4) - D_3^2 > 0. \tag{20}$$

Substituting the expressions for $D_i$ in terms of the model parameters $J_{ij}$, these stability conditions translate into the following explicit constraints:

$$\begin{aligned}
&-J_{11} - J_{33} > 0, \\
&J_{11}J_{24}J_{32}J_{43} - J_{11}J_{24}J_{33}J_{42} + J_{12}J_{21}J_{34}J_{43} - J_{12}J_{24}J_{31}J_{43} \\
&\quad + J_{12}J_{24}J_{33}J_{41} - J_{14}J_{21}J_{32}J_{43} + J_{14}J_{21}J_{33}J_{42} > 0, \\
&J_{11}J_{24}J_{32}J_{43} - J_{11}J_{24}J_{33}J_{42} + J_{12}J_{21}J_{34}J_{43} - J_{12}J_{24}J_{31}J_{43} \\
&\quad + J_{12}J_{24}J_{33}J_{41} - J_{14}J_{21}J_{32}J_{43} + J_{14}J_{21}J_{33}J_{42} > 0. \\
&D_1(D_2D_3 - D_1D_4) - D_3^2 > 0.
\end{aligned}$$

The last inequality represents a complicated algebraic condition that guarantees all eigenvalues have negative real parts. In view of its complexity, it is not explicitly expanded here; however, it must be satisfied to ensure stability.

### 3.5 Global Stability

To analyze the global stability properties of the endemic equilibrium, we construct an appropriate Lyapunov function. The analytical framework is developed as follows:

**Theorem 4.** Consider system (1) and assume that $0 < e_i < 1$ for $i = 1, 2, 3$. Let

$$E^* = (s_1^*, I^*, s_2^*, x^*)$$

be an endemic equilibrium of system (1) with strictly positive components. If

$$\alpha > \frac{kl^2}{4r}\frac{e_3}{e_1},$$

then $E^*$ is globally asymptotically stable in the interior of the feasible region

$$\Omega = \left\{(s_1, I, s_2, x) \in \mathbb{R}_+^4 : s_1 > 0,\ I > 0,\ s_2 > 0,\ x > 0\right\}.$$

*Proof.* Let

$$E^* = (s_1^*, I^*, s_2^*, x^*)$$

be the endemic equilibrium satisfying

$$s_1^* > 0, \qquad I^* > 0, \qquad s_2^* > 0, \qquad x^* > 0.$$

Consider the following Lyapunov function:

$$V(s_1, I, s_2, x) = \left(s_1 - s_1^* - s_1^* \ln\frac{s_1}{s_1^*}\right) + R_1\left(I - I^* - I^* \ln\frac{I}{I^*}\right) + R_2\left(s_2 - s_2^* - s_2^* \ln\frac{s_2}{s_2^*}\right) + R_3\left(x - x^* - x^* \ln\frac{x}{x^*}\right),$$

where $R_1$, $R_2$, and $R_3$ are positive constants to be determined later.

Differentiating $V$ with respect to $t$ along the solutions of system (1) gives

$$\frac{dV}{dt} = \left(1 - \frac{s_1^*}{s_1}\right)\frac{ds_1}{dt} + R_1\left(1 - \frac{I^*}{I}\right)\frac{dI}{dt} + R_2\left(1 - \frac{s_2^*}{s_2}\right)\frac{ds_2}{dt} + R_3\left(1 - \frac{x^*}{x}\right)\frac{dx}{dt}.$$

Through straightforward computation, it results:

$$\frac{dV}{dt} = -\frac{r}{k}(s_1 - s_1^*)^2 - R_2\alpha(s_2 - s_2^*)^2 + \left[-\frac{r}{k} + R_1\gamma - \gamma\right](s_1 - s_1^*)(I - I^*) + (R_3 e_1 - 1)b_1(s_1 - s_1^*)(x - x^*)$$

$$
\begin{aligned}
&+ (R_3e_2 - R_1)b_2(I - I^*)(x - x^*) \\
&+ (R_3e_3 - R_2)b_3(s_2 - s_2^*)(x - x^*) \\
&+ R_2 l\left[(s_2 - s_2^*)(s_1 - s_1^*)\right].
\end{aligned}
$$

To eliminate the cross-terms involving $(x - x^*)$, we choose the constants as follows:

$$
R_3 = \frac{1}{e_1}, \quad R_1 = \frac{e_2}{e_1}, \quad R_2 = \frac{e_3}{e_1}.
$$

Since $0 < e_i < 1$, we have $R_i > 0$ for all $i$. With this choice, $R_3e_1 - 1 = 0$, $R_3e_2 - R_1 = 0$, and $R_3e_3 - R_2 = 0$, so all terms containing $(x - x^*)$ vanish. The derivative simplifies to:

$$
\begin{aligned}
\frac{dV}{dt} = &-\frac{r}{k}(s_1 - s_1^*)^2 - \frac{e_3}{e_1}\alpha(s_2 - s_2^*)^2 + A^*(s_1 - s_1^*)(I - I^*) \\
&+ B^*(s_1 - s_1^*)(s_2 - s_2^*),
\end{aligned} \tag{21}
$$

where

$$
A^* = \gamma\left(\frac{e_2}{e_1} - 1\right) - \frac{r}{k}, \quad B^* = \frac{e_3}{e_1}l.
$$

Applying the Young's inequality

$$
\begin{aligned}
A^*(s_1 - s_1^*)(I - I^*) &\leq \frac{|A^*|}{2}\left(\varepsilon_1(s_1 - s_1^*)^2 + \frac{1}{\varepsilon_1}(I - I^*)^2\right), \\
B^*(s_1 - s_1^*)(s_2 - s_2^*) &\leq \frac{|B^*|}{2}\left(\varepsilon_2(s_1 - s_1^*)^2 + \frac{1}{\varepsilon_2}(s_2 - s_2^*)^2\right).
\end{aligned}
$$

where $\varepsilon_1, \varepsilon_2 > 0$ in (21) we obtain:

$$
\begin{aligned}
\frac{dV}{dt} \leqslant &-\frac{r}{k}(s_1 - s_1^*)^2 - \alpha(s_2 - s_2^*)^2 + A^*\left(\frac{(s_1 - s_1^*)^2}{2} + \frac{(I - I^*)^2}{2}\right) \\
&+ B^*\left(\frac{(s_2 - s_2^*)^2}{2} + \frac{(s_1 - s_1^*)^2}{2}\right).
\end{aligned}
$$

Choosing $\varepsilon_1 = \frac{2r}{|A^*|k}$ and $\varepsilon_2 = \frac{2r}{|B^*|k}$ to balance the coefficients of $(s_1 - s_1^*)^2$, we have:

$$
\frac{dV}{dt} \leq -\frac{r}{2k}(s_1 - s_1^*)^2 - \left(\frac{e_3}{e_1}\alpha - \frac{B^{*2}k}{4r}\right)(s_2 - s_2^*)^2 - \frac{A^{*2}k}{4r}(I - I^*)^2. \tag{22}
$$

Since $\frac{A^{*2}k}{4r} > 0$, the coefficient of $(I - I^*)^2$ is negative, and the coefficient of $(s_1 - s_1^*)^2$ is also negative. Thus, a sufficient condition for $\frac{dV}{dt} \leq 0$ is:

$$
\alpha > \frac{kl^2}{4r} \cdot \frac{e_3}{e_1}.
$$

Under this condition, $\frac{dV}{dt} \leq 0$ . Therefore, By LaSalle's invariance principle, $E^*$ is globally asymptotically stable in $\Omega$. □

## 4 Sensitivity Analysis

To identify the most influential parameters affecting disease dynamics in the predator-prey system, a global sensitivity analysis was performed using Latin Hypercube Sampling (LHS) combined with the Partial Rank Correlation Coefficient (PRCC) method [15]. This well-established approach provides a comprehensive assessment of how parameter variations, both individually and through their interactions, influence the steady-state infected population ($I^*$). The LHS–PRCC framework has been widely used in epidemiological and ecological models due to its efficiency and robustness for exploring complex and nonlinear parameter spaces.

**Table 2:** PRCC values for the parameters of model (1).

| **Parameter** | $\Lambda$ | $r$ | $k$ | $l$ | $\alpha$ | $\lambda$ | $\mu$ |
|---|---|---|---|---|---|---|---|
| **PRCC** | 0.1037 | 0.5873 | 0.9461 | 0.0668 | 0.1237 | 0.1061 | -0.9271 |
| **Parameter** | $b_1$ | $b_2$ | $b_3$ | $\gamma$ | $e_1$ | $e_2$ | $e_3$ |
| **PRCC** | 0.1472 | 0.1335 | 0.1221 | 0.8963 | 0.1096 | 0.1230 | 0.1013 |

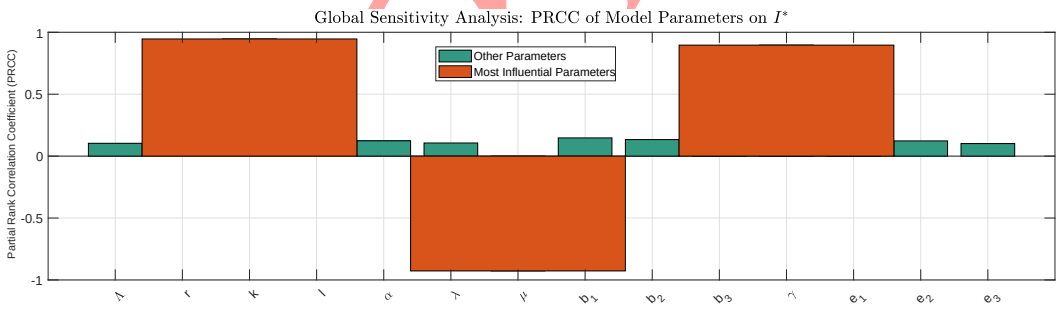


**Figure 2:** Global Sensitivity Analysis: PRCC of parameters on the steady-state infected population ($I^*$). The figure highlights the primary targets ($\gamma$, $\mu$, $k$) for potential intervention strategies to control disease spread.

The results in Table 2 and Figure 2 indicate that carrying capacity $k$ (PRCC = 0.9461) and disease transmission rate $\gamma$ (PRCC = 0.8963) are the most influential positive parameters affecting $I^*$. Increases in $k$ or $\gamma$ substantially elevate the infected population at equilibrium. The prey growth rate $r$ also contributes positively (PRCC = 0.5873), though its effect is moderate compared to $k$ and $\gamma$.

Conversely, the disease-induced removal rate $\mu$ has a strong negative effect (PRCC = $-0.9271$), highlighting its crucial role in reducing the prevalence of infection in the system. Other parameters, including environmental and predator–prey interaction coefficients ($b_1, b_2, b_3, e_1, e_2, e_3, \Lambda, \alpha, l, \lambda$), exhibit relatively minor effects (PRCC $\approx$ 0.1–0.15).

These findings are consistent with previous local (OAT) sensitivity analyses, confirming that $\gamma$ and $\mu$ are key parameters for disease management. The global analysis additionally accounts for parameter interactions and system nonlinearity, providing a robust and comprehensive understanding of model sensitivity.

## 5 Optimal Control Formulation

In this study, we consider two time-dependent control strategies: $u_1(t)$ representing isolation management, and $u_2(t)$ representing treatment administration. These controls are implemented as piecewise continuous (PC) functions over the time interval $[0, T]$, with the admissible range $0 \leq u_1(t), u_2(t) \leq 1$ for all $t \in [0, T]$.

(1) The isolation control $u_1(t) \in [0, 1]$ modulates disease transmission by reducing the term $\gamma S_1 I$ to $(1-u_1(t))\gamma S_1 I$. Here, the factor $(1-u_1(t))$ quantifies the residual transmission risk, where $u_1(t) = 0$ corresponds to no isolation (natural transmission), and $u_1(t) = 1$ corresponds to perfect isolation (complete suppression of transmission). The control thus captures isolation efficacy on a continuous spectrum.

(2) The treatment control $u_2(t) \in [0, 1]$ enhances the recovery rate by transferring infected individuals $I$ back to the susceptible class $S_1$ at rate $u_2(t)I$, while simultaneously reducing the infected population. The extremes $u_2(t) = 0$ and $u_2(t) = 1$ correspond to no treatment and maximal treatment intensity, respectively, with $u_2(t)$ representing the treatment efficacy.

(3) Collectively, the controls $u_1(t)$ and $u_2(t)$ influence the disease dynamics by reducing transmission and accelerating recovery, respectively. Both controls belong to the admissible set

$$\mathcal{U} = \{(u_1, u_2) \in PC[0, T] \mid 0 \leq u_i(t) \leq 1, \quad \forall t \in [0, T]\}, \tag{23}$$

ensuring biological feasibility throughout the epidemic horizon.

Consequently, the system dynamics under control become

$$\begin{aligned}
\frac{ds_1}{dt} &= rs_1\left(1 - \frac{s_1 + I}{k}\right) - b_1 s_1 x - \gamma(1-u_1)s_1 I + u_2 I, \\
\frac{dI}{dt} &= \gamma(1-u_1)s_1 I - b_2 I x - \mu I - u_2 I, \\
\frac{ds_2}{dt} &= \Lambda - \alpha s_2 - b_3 s_2 x + l s_1,
\end{aligned} \tag{24}$$

$$\frac{dx}{dt} = -\lambda x + e_1 b_1 s_1 x + e_2 b_2 I x + e_3 b_3 s_2 x.$$

The objective is to minimize both the infected population and the costs associated with control implementation via the cost functional

$$\min_{u_1,u_2} \mathcal{J} = \int_0^T \left[ AI(t) + \frac{1}{2}\left(B_1 u_1^2(t) + B_2 u_2^2(t)\right) \right] dt, \tag{25}$$

where $A, B_1, B_2 \geq 0$ are weight parameters and $T > 0$ is the fixed terminal time.

**Theorem 5.** By Fleming and Rishel's theorem [8, 18], the existence of optimal controls $(u_1^*, u_2^*) \in \mathcal{U}$ is guaranteed because:

1. The control set $\mathcal{U}$ is convex and closed;
2. The state system is bounded above by a linear function;
3. The integrand of $J$ is convex in the controls;
4. The state variables remain non-negative on $[0, T]$.

*Proof.* It is clear that the linear combination of them is piecewise, also the limit of a sequence of piecewise functions is piecewise, too. Therefore $\mathcal{U}$ is convex and closed.

The integrand of the cost functional $J$ is a polynomial function of the controls $u_1$ and $u_2$ (typically quadratic with positive coefficients, e.g., $u_1^2 + u_2^2$). Polynomials of piecewise continuous functions are piecewise continuous, and since the quadratic form is convex on $\mathbb{R}^2$, the integrand is convex in $(u_1, u_2)$ over the convex set $\mathcal{U}$.

The non-negativity and boundedness of the state variables in the original dynamics (1) have been established in Theorems 2 and 3. Because the admissible controls $u_1, u_2$ are bounded and non-negative, the right-hand side of the state equations grows at most linearly in the state variables. Consequently, the state variables in the costate system (24) are also non-negative and bounded.

All conditions of the Fleming–Rishel theorem are therefore satisfied, guaranteeing the existence of optimal controls $(u_1^*, u_2^*) \in \mathcal{U}$. □

Applying Pontryagin's Maximum Principle (PMP), the Hamiltonian $\mathcal{H}$ associated with the controlled system (24) is

$$\mathcal{H} = AI(t) + \frac{1}{2}\left(B_1 u_1^2(t) + B_2 u_2^2(t)\right) + \sum_{i=1}^{4} \lambda_i(t) f_i(t), \tag{26}$$

where

$$f_1 = r s_1 \left(1 - \frac{s_1 + I}{k}\right) - b_1 s_1 x - \gamma(1 - u_1) s_1 I + u_2 I,$$

$$
\begin{aligned}
f_2 &= \gamma(1-u_1)s_1 I - b_2 I x - \mu I - u_2 I,\\
f_3 &= \Lambda - \alpha s_2 - b_3 s_2 x + l s_1,\\
f_4 &= -\lambda x + e_1 b_1 s_1 x + e_2 b_2 I x + e_3 b_3 s_2 x,
\end{aligned}
$$

and $\lambda_i(t)$, $i = 1, \ldots, 4$, are the adjoint variables satisfying the necessary conditions:

$$
\begin{aligned}
\lambda_1' &= -\left[\lambda_1\left(r\left(1-\frac{2s_1+I}{k}\right) - b_1 x - \gamma(1-u_1)I\right) + \lambda_2\gamma(1-u_1)I + \lambda_4 e_1 b_1 x\right],\\
\lambda_2' &= -\left[A + \lambda_1\left(-\frac{r s_1}{k} - \gamma(1-u_1)s_1 + u_2\right) + \lambda_2\left(\gamma(1-u_1)s_1 - b_2 x - \mu - u_2\right)\right.\\
&\quad \left. + \lambda_3 l s_2 + \lambda_4 e_2 b_2 x\right],\\
\lambda_3' &= -\left[\lambda_3(-\alpha - b_3 x) + \lambda_4 e_3 b_3 x\right],\\
\lambda_4' &= -\left[-\lambda_1 e_1 b_1 s_1 - \lambda_2 e_2 b_2 I - \lambda_3 e_3 b_3 s_2 + \lambda_4(-\lambda + e_1 b_1 s_1 + e_2 b_2 I + e_3 b_3 s_2)\right].
\end{aligned}
\tag{27}
$$

The transversality conditions are given by

$$
\lambda_i(T) = 0, \quad i = 1, 2, 3, 4.
$$

The characterization of optimal controls $u_1^*(t)$ and $u_2^*(t)$ is

$$
u_1^*(t) = \min\left\{1, \max\left\{0, \frac{\gamma s_1(t) I(t)\left(\lambda_2(t) - \lambda_1(t)\right)}{B_1}\right\}\right\}, \tag{28}
$$

$$
u_2^*(t) = \min\left\{1, \max\left\{0, \frac{I(t)\left(\lambda_2(t) - \lambda_1(t)\right)}{B_2}\right\}\right\}. \tag{29}
$$

## 6 Numerical Simulation

For the numerical simulation of the disease-affected predator-prey model, the ode45 function in MATLAB was employed. This function is based on the fourth-fifth order Runge-Kutta method (RK45), which provides high accuracy for solving nonlinear first-order differential systems and allows automatic step-size control. The control variables, isolation $(u_1)$ and treatment $(u_2)$, were applied dependent on the infected population to simultaneously evaluate their effects on healthy, infected, and predator populations.

The parameter values employed in this manuscript are drawn from the references given in Table 3, and their specific numerical values are reported in Table 4. These values are selected to simultaneously satisfy the local stability conditions derived in Section 3 and to remain within biologically plausible ranges, consistent with standard eco-epidemiological literature [2, 3, 8, 11, 18, 21]

**Table 3:** References for the biological interpretation of model parameters.

| Parameter | Interpretation | Reference(s) |
|---|---|---|
| $r, k, \Lambda, \alpha$ | Growth rates, carrying capacity, inflow, and mortality | [2] |
| $\gamma, \mu$ | Infection rate and disease-induced mortality | [21] |
| $b_i, e_i$ | Predation rates and conversion efficiencies | [3] |
| $l, \lambda$ | Indirect effect strength and predator mortality | [11] |
| $A, B_1, B_2$ | Cost-functional weights | [8, 18] |



**Table 4:** Parameter values used for the equilibrium points $E_1$–$E_6$ of model (1).

| Parameter | $E_1$ | $E_2$ | $E_3$ | $E_4$ | $E_5$ | $E_6$ |
|---|---|---|---|---|---|---|
| $\Lambda$ | 1000 | 0.375 | 0.5 | 0.4 | 0.24 | 0.5 |
| $r$ | 0.02 | 1.2 | 0.5 | 1.2 | 0.25 | 0.6 |
| $k$ | 2000 | 0.2 | 0.2 | 0.2 | 0.6 | 1.5 |
| $l$ | 50 | 0.90 | 0.9 | 0.5 | 0.7 | 0.2 |
| $\alpha$ | $10^{-6}$ | 0.60 | 0.50 | 0.2 | 0.9 | 0.3 |
| $\lambda$ | 0.01 | 0.55 | 0.2 | 0.6 | 1.0 | 0.2 |
| $\mu$ | 2 | 0.80 | 0.8 | 0.4 | 0.4 | 0.1 |
| $b_1$ | 1 | 1.0 | 0.82 | 0.9 | 0.7 | 0.2 |
| $b_2$ | 1.2 | 1.2 | 1.1 | 1.2 | 0.8 | 0.2 |
| $b_3$ | 0.1 | 0.40 | 0.50 | 0.7 | 0.40 | 0.3 |
| $\gamma$ | 0 | 0.40 | 0.40 | 0.40 | 0.90 | 1 |
| $e_1$ | 0 | 0.70 | 0.70 | 0.70 | 0.70 | 0.6 |
| $e_2$ | 0 | 0.70 | 0.70 | 0.70 | 0.70 | 0.3 |
| $e_3$ | 0 | 0.70 | 0.70 | 0.70 | 0.70 | 0.7 |

### 6.1 Numerical Simulation of the Equilibrium Point $E_5$

This section presents numerical simulations of the predator-prey model around the infectious equilibrium point $E_5 = (s_1^*, I^*, s_2^*, 0)$. The parameter values used are those listed for $E_5$ in the fifth column of Table 4.

The initial condition vector is set to $[s_1, I, s_2, x] = [0.7, 0.1, 0.8, 0.1]$, and the simulation is performed over the time interval $[0, 40]$.

Figure 3 illustrates the time evolution of the infected prey population $I$, susceptible prey $s_1$, susceptible secondary prey $s_2$, and predator population $x$ for both controlled and uncontrolled cases. Results confirms the local stability behavior near $E_5$ and demonstrates in absence of predator population.

**Interpretation of Figure 3:** In the uncontrolled case (blue dashed line), the infected prey population $I$ initially increases from 0.1, overshoots slightly, and converges to $I^* \approx 0.107$ after $t \approx 20$; under optimal controls (red solid line), $I$ rises more slowly, peaks near 0.09, and stabilizes at a value approximately 10% lower than the uncontrolled equilibrium, demonstrating the effectiveness of combined isolation and treatment. The susceptible first prey $s_1$ starts at 0.7: uncontrolled, it declines to $s_1^* \approx 0.67$, while under control it remains higher throughout, settling near 0.69 due to reduced infection pressure and return of treated individuals to the susceptible class. The secondary prey $s_2$, being disease-free and competitively superior, remains largely unaffected, with both trajectories converging to $s_2^* \approx 0.95$, indicating regulation primarily by its own growth parameters rather than by infection status. The predator population $x$ decays to zero in both scenarios (consistent with the predator-free equilibrium $E_5$), with slightly faster decay under control due to reduced prey biomass. Overall, Figure 3 confirms local stability near $E_5$ and shows that the applied controls successfully reduce infection without destabilizing the system or inducing predator persistence. Importantly, the optimal control strategy achieves a substantial reduction in the total cost functional $\mathcal{J}$ defined in (25), decreasing it by approximately $84.0\%$ compared with the uncontrolled scenario, which highlights the economic and biological efficiency of the dual interventions even when the predator is absent.

### 6.2 Numerical Simulation of the Equilibrium Point $E_6$

We performed numerical simulations of the predator-prey dynamical system at the infectious equilibrium point $E_6$ to illustrate the effect of controls in presence of disease population. The parameter set corresponding to $E_6$ is given in the sixth column of the Table 4. The initial conditions were set as:

$$[s_1, I, s_2, x] = [0.3, 0.1, 0.4, 0.2].$$

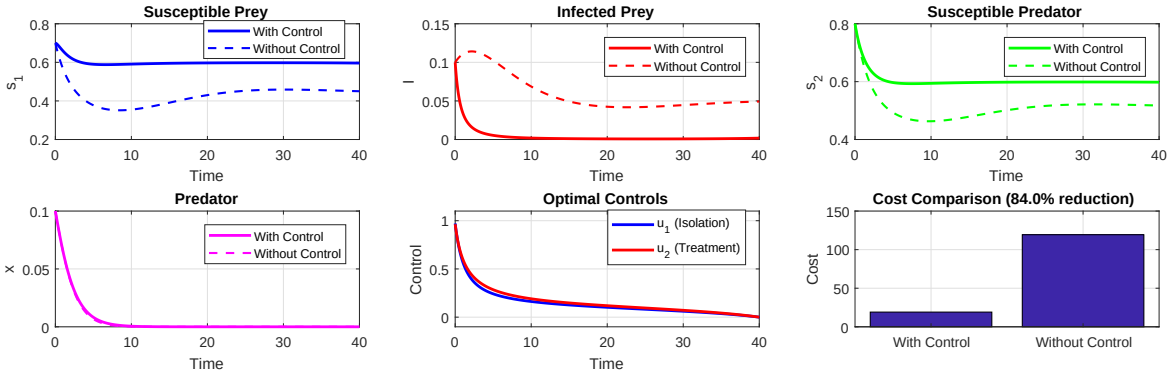


**Figure 3:** Dynamics of the system near the predator-free endemic equilibrium $E_5$ under optimal control, compared with the uncontrolled case.

Simulations were conducted over the time interval $[0, 80]$ both without control and with time-dependent piecewise controls $u_1(t)$ and $u_2(t)$.

Figure 4 compares the trajectories of infected prey $I$, susceptible prey $s_1$, susceptible secondary prey $s_2$, and predator population $x$ under controlled and uncontrolled dynamics. This numerical approach demonstrates the effects of controls on infectious prey and predator populations, providing insight into potential management strategies for disease spread in ecological systems.

*Interpretation of Figure 4*: In the uncontrolled case (blue dashed line), the infected prey population $I$ exhibits damped oscillations and converges to a positive endemic equilibrium $I^* \approx 0.18$; after controls activate at $t = 10$ (red solid line), the infected population declines sharply, dropping by approximately 25% within 20 time units and stabilizing at a significantly lower level, reflecting the synergistic effect of reducing transmission $(u_1)$ and removing infected individuals $(u_2)$. The susceptible first prey $s_1$ starts at 0.3 and increases noticeably under control compared to the uncontrolled trajectory due to two factors: reduced infection transmission leaves more susceptible individuals, and treated individuals re-enter the $s_1$ class, which contributes to stabilizing the predator population by providing a healthier prey base. The secondary prey $s_2$, being disease-free and competitively superior, remains stable in both scenarios, but under control shows a slight increase (approximately $5 - 8\%$) because the predator's pressure on $s_1$ and $I$ shifts the predator's diet slightly, indirectly benefiting $s_2$ as an important ecological consequence of disease management. The predator population $x$ persists at a moderate equilibrium in the uncontrolled case; under control, it initially dips slightly due to reduced infected prey availability but then recovers and stabilizes at a level comparable to or slightly higher than the uncontrolled case, indicating that control strategies do not harm the predator but instead promote a healthier predator-prey balance by sustaining the susceptible prey base. Regarding the control profiles (inset), both $u_1$ and $u_2$ are active primarily during

the early intervention period (from $t = 10$ to approximately $t = 30$), after which they decay to lower values; isolation $(u_1)$ peaks near 0.7, while treatment $(u_2)$ peaks near 0.5, suggesting that a combination of moderate isolation and treatment is sufficient to achieve long-term disease reduction without incurring excessive control costs. Furthermore, the optimal control reduces the overall cost functional $\mathcal{J}$ by approximately $94.2\%$ relative to the no-control case, confirming the strong synergistic benefit of combining isolation and treatment in the presence of a persistent predator. Overall, Figure 4 demonstrates that the optimal control strategy effectively reduces infection prevalence, enhances healthy prey populations, and maintains predator persistence, providing strong evidence that targeted interventions can mitigate disease impacts while preserving ecosystem structure.

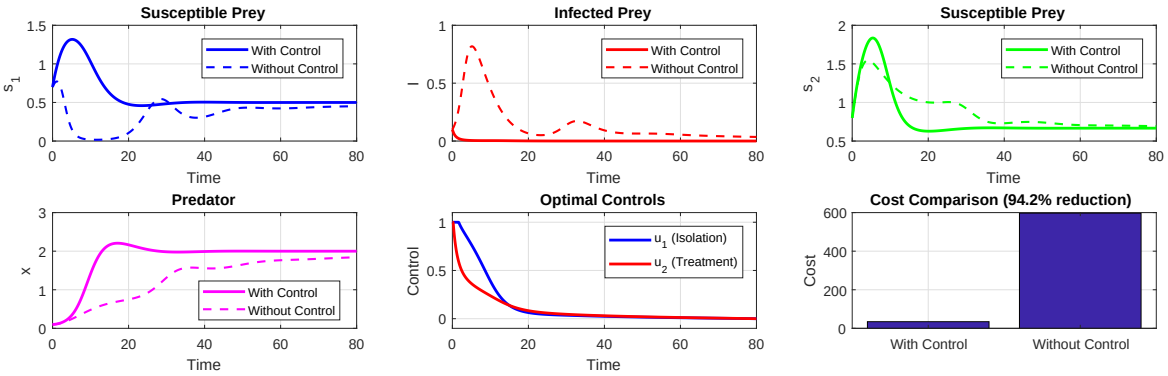


**Figure 4:** Dynamics of the system near the coexistence equilibrium $E_6$ under optimal control, compared with the uncontrolled case.

## 7 Conclusion

This study explored the dynamics of a predator-prey system comprising two prey species and one predator, incorporating an infection in one of the prey populations and two time-dependent control interventions. Through analytical and numerical methods, we investigated the existence and stability of all possible equilibrium points, including free-disease and endemic states. Theoretical analysis confirmed that the system remains bounded and exhibits global asymptotic stability under specific parameter conditions, verified through Lyapunov-based criteria and simulation results. The sensitivity analysis revealed that the carrying capacity $(k)$, infection rate $(\gamma)$, and disease-induced mortality $(\mu)$ are the most influential parameters governing infection persistence. This finding suggests that environmental resource control and reduction of disease transmissibility are critical for ecosystem health. The optimal control analysis demonstrated that combining isolation $(u_1)$ and treatment $(u_2)$ effectively reduces infection prevalence, en-

hances healthy prey populations, and stabilizes predator density compared with single or uncontrolled scenarios. From a biological perspective, the results highlight how disease transmission can significantly alter interspecies balance, yet well-designed control measures can restore ecological stability. The integration of stability analysis, sensitivity assessment, and optimal control provides a comprehensive framework linking theoretical predictions to practical ecosystem management.

*Limitations and Future Work* – While the proposed model offers valuable insights into predator-prey dynamics under dual disease interventions, several limitations warrant acknowledgment. The use of mass-action incidence $\gamma s_1 I$ assumes homogeneous mixing and may not capture saturation or behavioral effects; future work will explore more general incidence functions. The absence of spatial or diffusion effects despite being highlighted as a motivational gap-restricts the model's applicability to heterogeneous environments, and incorporating reaction-diffusion or patch-structured frameworks is a natural extension. Moreover, the parameter sets, although drawn from literature, lack validation against real field or experimental data, underscoring the need for empirical calibration. Planned extensions also include fractional-order dynamics and stochastic perturbations to account for memory effects and environmental noise, as well as incorporating Allee effects or prey refuge, thereby enhancing ecological realism and the robustness of control recommendations.



## Declarations

### Availability of Supporting Data

The data that support the findings of this study are available from the corresponding author upon reasonable request. Due to organizational confidentiality, the data are not publicly available.

### Funding

The authors received no specific funding for this research.

### Conflict of Interest

The authors declare that they have no known competing financial interests or personal relationships that could have influenced the work reported in this paper.

### Authors Contributions

**Mahnaz Abedini** contributed to the conceptualization, methodology, software and validation, formal analysis, writing– review and editing, and visualization. **Gorbanali Haghighatdoost** contributed to the conceptualization, software and validation, formal

analysis, investigation, writing– review and editing, and visualization. **Hossein Kheiri** contributed to the conceptualization, methodology, software and validation, resources, writing– original draft preparation, writing– review and editing, visualization, supervision, and project administration. All authors have read and approved the published version of the manuscript.

**Artificial Intelligence Statement**

Artificial intelligence (AI) tools, including large language models, were used solely for language editing and improving readability. AI tools were not used for generating ideas, performing analyses, interpreting results, or writing the scientific content. All scientific conclusions and intellectual contributions were made exclusively by the authors.

**Publisher's Note**

The publisher remains neutral regarding jurisdictional claims in published maps and institutional affiliations.



## References

[1] Ahmed, E., El-Sayed, A.M.A., El-Saka, H.A.A. (2006). "On some Routh-Hurwitz conditions for fractional order differential equations and their applications in Lorenz, Rössler, Chua and Chen systems". *Physics Letters A*, 358(1), 1-4. https://doi.org/10.1016/j.physleta.2006.04.087

[2] Brauer, F., Castillo-Chávez, C. (2012). "Mathematical Models in Population Biology and Epidemiology". *Texts in Applied Mathematics*, Volume 40. https://doi.org/10.1007/978-1-4614-1686-9

[3] Chattopadhyay, J., Srinivasu, P. D. N., Bairagi, N. (2003). "Pelicans at risk in Salton Sea: An eco-epidemiological model-II". *Ecological Modelling*, 167(1-2), 199-211. https://doi.org/10.1016/S0304-3800(03)00187-X

[4] Chen, J.T., et al. (2025). "Bottom-up and top-down effects combine to drive predator–prey interactions in a forest biodiversity experiment". *Journal of Animal Ecology*, 94, 2035-2046. https://doi.org/10.1111/1365-2656.70103

[5] Davarian, N., Heydari, A., Hashemi Mehne, S.H., Heydari, A.A. (2025). "The investigation of stability and optimal control of the multigroup COVID-19 epidemic model in Iran". *Journal of Mathematical Extension*, 19(1), 1-32. https://doi.org/10.30495/JME.2025.3165

[6] Davarian, N., Heydari, A., Hashemi Mehne, S.H. (2025). "Presenting a multi-group model and optimal control of an infectious disease in Iran". *Journal of Operational Research in Its Applications*, 22(1), 107-123.

[7] Du, R., Liang, X., Na, Y., Xu, F. (2025). "Optimal control of an eco-epidemiological reaction-diffusion model". *Mathematics*, 13(13), 2069. https://doi.org/10.3390/math13132069

[8] Fleming, W.H., Rishel, R.W. (1975). "Deterministic and stochastic optimal control". *Springer-Verlag*. https://doi.org/10.1007/978-1-4612-6380-7

[9] Gómez-Hernández, E.A., et al. (2024). "Eco-epidemiological predator–prey models: A review of models in ordinary differential equations". *Ecological Complexity*, 57, 101071. https://doi.org/10.1016/j.ecocom.2023.101071

[10] Greenhalgh, D., Khan, Q.J.A., Pettigrew, J.S. (2017). "An eco-epidemiological predator–prey model where predators distinguish between susceptible and infected prey". *Mathematical Methods in the Applied Sciences*, 40(1), 146-166. https://doi.org/10.1002/mma.3974

[11] Kar, T.K., Ghosh, B. (2012). "Sustainability and optimal control of an exploited prey predator system through provision of alternative food to predator". *Biosystems*, 109(2), 220-232. https://doi.org/10.1016/j.biosystems.2012.02.003

[12] Kebedow, K., Cheru, S.L., Ega, T.T. (2025). "Optimal Control Strategies in a Diseased Prey–Predator Model With Holling Type-II Dynamics". *Journal of Applied Mathematics*, 5535536, 17 pages. https://doi.org/10.1155/jama/5535536

[13] Kheiri, H., Jafari, M. (2018). "Optimal control of a fractional-order model for the HIV/AIDS epidemic". *International Journal of Biomathematics*, 11(07), 1850086. https://doi.org/10.1142/S1793524518500869

[14] Lennox, R.J., et al. (2025). "The role of habitat in predator–prey dynamics with applications to restoration". *Restoration Ecology*, 33(8), e14354. https://doi.org/10.1111/rec.14354

[15] Marino, S., Hogue, I.B., Ray, C.J., Kirschner, D.E. (2008). "A methodology for performing global uncertainty and sensitivity analysis in systems biology". *Journal of Theoretical Biology*, 254(1), 178-196. https://doi.org/10.1016/j.jtbi.2008.04.011

[16] Mekonen, K.G., Bezabih, A.F., Rao, K.P. (2024). "Mathematical modeling of infectious disease and prey-predator interaction with optimal control". *International Journal of*

*Mathematics and Mathematical Sciences*, 2024(1), Article 5444627. https://doi.org/10.1155/2024/5444627

[17] Mukhopadhyay, S., Bhattacharyya, S. (2009). "Role of predator switching in an eco-epidemiological model with disease in the prey". *Ecological Modelling*, 220(7), 931-939. https://doi.org/10.1016/j.ecolmodel.2009.01.016

[18] Naidu, D.S. (2003). "Optimal control systems". *CRC Press*. https://doi.org/10.1201/9781315214429

[19] Sarkar, K., Khajanchi, S. (2022). "An eco-epidemiological model with the impact of fear". *Chaos: An Interdisciplinary Journal of Nonlinear Science*, 32(8), 083126. https://doi.org/10.1063/5.0099584

[20] Teschl, G. (2012). "Ordinary differential equations and dynamical systems". *American Mathematical Society*, 140. https://doi.org/10.1090/gsm/140

[21] Venturino, E. (2002). "Epidemics in predator–prey models: disease in the predators". *Mathematical Medicine and Biology: A Journal of the IMA*, 19(3), 185-205. https://doi.org/10.1093/imammb/19.3.185

[22] Zhang, X., Wang, G., Zhu, H. (2020). "Optimal control of a diffusive eco-epidemiological predator-prey model". *International Journal of Biomathematics*, 13(7), 2050065. https://doi.org/10.1142/S1793524520500655

**Authors Bio-sketches**

**Mahnaz Abedini** is a PhD student at Azarbaijan Shahid Madani University, majoring in Dynamical Systems. She Completed her Master's degree in Dynamical Systems at the same university (Azarbaijan Shahid Madani University).

**Gorbanali Haghighatdoost** is a Full Professor of Mathematics at Azarbaijan Shahid Madani University, specializing in Geometry of Dynamical Systems. He received his Ph.D. in Geometry from Moscow State University and his M.Sc. in Geometry from the University of Tabriz. His current research interests encompass geometry, dynamical systems, and mathematical modeling with applications in ecological and epidemiological systems.

**Hossein Kheiri** is a Full Professor of Applied Mathematics at the University of Tabriz, specializing in Dynamical Systems and Mathematical Biology. He received his Ph.D. in Dynamical Systems and his M.Sc. in Applied Mathematics, both from the University of

Tabriz. His current research interests include dynamical systems, mathematical modeling in biological problems, optimal control, and machine learning. Corresponding author. Email: h-kheiri@tabrizu.ac.ir